IR + Raman - IR- and Raman-Spectroscopy

Protocol for the PC 2 lab course by

Vincent Kümmerle & Elvis Gnaglo & Julian Brügger

University of Stuttgart

authors:	Vincent Kümmerle, 3712667 st187541@stud.uni-stuttgart.de
	Elvis Gnaglo, 3710504 st189318@stud.uni-stuttgart.de
	Julian Brügger, 3715444 st190050@stud.uni-stuttgart.de
group number:	A05
date of experiment:	21.01.2026
supervisor:	Mansha Shafquath
submission date:	January 26, 2026

Abstract:

Contents

1 Theory

1.1 IR-Spectroscopy

When a dipolar molecule is exposed to an electromagnetic field the partially positive charged atom is pushed along the direction of the magnetic field lines. So if a molecule is exposed to an oscillating field, that oscillates at the natural vibration frequency of said molecule, the molecule will be in an excited vibrational state.

1.2 Raman-Spectroscopy

1.3 DFT-Calculations

[1]

2 Procedure

To simulate and calculate the vibrational normal modes, the program `Avogadro2` was used. The structures of the molecules methane, chloromethane, dichloromethane, dibromomethane, chloroform, deuterated chloroform, tetrachloromethane and tetrachloroethylene were built, their geometry was optimized and the optimized coordinates were used to calculate the vibrational modes with the `ORCA` software, resulting in a list of IR and Raman frequencies and intensities for each molecule.
In the experimental part, the Raman spectra of dichloromethane, dibromomethane, chloroform, deuterated chloroform, tetrachloromethane and tetrachloroethylene were measured and analysized with the `WPenlighten` software. The IR spectra of dichloromethane, dibromomethane, chloroform and tetrachloroethylene were measured using an ATR spectrometer and analysized with the `Opus` software.

3 Results and Analysis

3.1 Methane

3.1.1 IR

The simulated vibrational modes of methane are summarized in Table 1 with the corresponding wavenumber, intensity and vibration type of each mode.

Tab. 1: Listed are the simulated wavenumbers and intensities of the IR signals of CH_4 with the corresponding type of the vibrational mode.

Signal	Wavenumber $\tilde{\nu}$ / cm^{-1}	Intensity / $KM \cdot mol^{-1}$	Vibration type
1	1313.45	13.30	asym. bending
2	1313.68	13.25	asym. bending
3	1313.73	13.25	asym. bending
4	1530.79	0	sym. bending
5	1531.05	0	sym. bending
6	3019.38	0	sym. stretching
7	3152.03	17.69	asym. stretching
8	3152.33	17.64	asym. stretching
9	3152.45	17.64	asym. stretching

As can be seen in Table 1, only the asymmetric bending and stretching modes are IR-active, while the symmetric bending and stretching modes are IR-inactive. Furthermore, the asymmetric stretching mode shows the highest wavenumber among the IR-active modes, meaning it requires the most energy to be excited.

3.1.2 Raman

The simulated Raman-active vibrational modes of methane are summarized in **??** with the corresponding wavenumber, Raman intensity and vibration type of each mode.

Tab. 2: Listed are the simulated wavenumbers and intensities of the Raman signals of CH_4 with the corresponding type of the vibrational mode.

Mode	Raman shift $\Delta\tilde{\nu}$ / cm^{-1}	Raman intensity / $Å^4 \cdot amu^{-1}$	Vibration type
1	1313.38	1.64419	asym. bending
2	1313.61	1.6422	asym. bending
3	1314.1	1.6484	asym. bending
4	1531.00	27.4565	sym. bending
5	1531.09	27.449	sym. bending
6	3019.41	145.177	sym. stretching
7	3150.24	62.8181	asym. stretching
8	3150.27	62.8724	asym. stretching
9	3150.79	62.8305	asym. stretching

In contrast to the IR spectrum, both the symmetric bending and stretching modes are Raman-active. The symmetric stretching mode shows the highest Raman intensity among all vibrational modes, indicating that it is most prominent mode to be observed in a Raman spectrum.

3.2 Chloromethane

3.2.1 IR

The simulated vibrational modes of methane are summarized in Table 3 with the corresponding wavenumber, intensity and vibration type of each mode.

Tab. 3: Listed are the simulated wavenumbers and intensities of the vibrational modes of CH_3Cl.

Mode	Wavenumber $\tilde{\nu}$ / cm^{-1}	Intensity / km mol^{-1}	vibration type
1	725.98	23.93	C−Cl stretch
2	1010.21	3.13	rocking
3	1010.42	3.11	rocking
4	1361.61	14.72	scissoring
5	1455.99	6.46	twisting
6	1456.14	6.47	twisting
7	3057.12	21.81	sym. stretching
8	3170.28	6.28	asym. stretching
9	3170.74	6.27	asym. stretching

The table shows that all types of vibrations are IR active but the C−Cl stretching mode as well as the scissoring mode and symmetrical stretching mode are the most intense ones.

3.2.2 Raman

The simulated Raman-active vibrational modes of methane are summarized in Table 4 with the corresponding wavenumber, Raman intensity and vibration type of each mode.

Tab. 4: Listed are the simulated Raman shifts and intensities of the vibrational modes of CH_3Cl.

Mode	Raman Shift $\Delta\tilde{\nu}$ / cm^{-1}	Raman intensity / $Å^4$ amu^{-1}	vibration type
1	725.96	12.69	C−Cl stretch
2	1008.86	6.56	rocking
3	1010.02	6.53	rocking
4	1361.35	3.48	scissoring
5	1455.81	16.49	twisting
6	1456.34	16.50	twisting
7	3056.94	134.62	sym. stretching
8	3169.78	66.78	asym. stretching
9	3170.01	66.72	asym. stretching

The comparison to the IR table shows that all vibrational modes are also raman active but the most intense ones are now the stretching modes, with the symmetrical stretching being the most prominent one.

3.3 Dichloromethane

3.3.1 IR

The measured IR spectrum of dichloromethane is shown in Figure 1, plotting the intensity of the absorption against the wavenumber $\tilde{\nu}$.

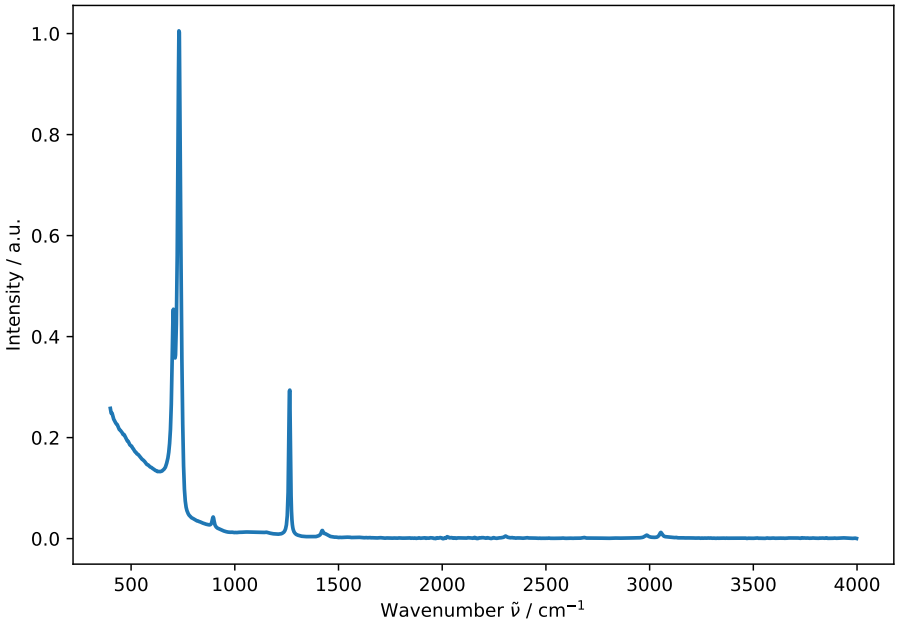

Fig. 1: Measured IR spectrum of dichloromethane.

By visual inspection of the IR spectrum in Figure 1, five absorption signals can be identified, which are listed with their corresponding wavenumbers and intensities in Table 5.

Tab. 5: Listed are the measured wavenumbers and intensities of the IR signals of CH_2Cl_2 with the corresponding type of the vibrational mode.

Signal	Wavenumber $\tilde{\nu}$ / cm^{-1}	Intensity / a.u.	Vibration type
1	704.00	0.45	sym. stretching
2	730.53	1.01	asym. stretching
3	895.82	0.04	rocking
4	1265.17	0.29	wagging
5	1422.29	0.02	scissoring

The simulated vibrational modes of dichloromethane are summarized in Table 6 with the corresponding wavenumber, intensity and vibration type of each mode.

Tab. 6: Listed are the simulated wavenumbers and intensities of the IR signals of CH_2Cl_2 with the corresponding type of the vibrational mode.

Mode	Wavenumber $\tilde{\nu}$ / cm^{-1}	Intensity / $KM \cdot mol^{-1}$	Vibration type
1	277.23	0.64	-
2	703.86	14.19	sym. stretching
3	733.80	137.83	asym. stretching
4	889.17	1.20	rocking
5	1153.54	0.00	-
6	1272.86	41.21	wagging
7	1441.46	0.01	scissoring
8	3107.43	9.81	sym. stretching
9	3194.30	0.64	asym. stretching

As can be seen in Table 6, the most intense IR-active modes are found at wavenumbers of 733.80 cm^{-1} and 1272.86 cm^{-1}, which correspond well to the measured signals at 730.53 cm^{-1} for the asymmetric stretching mode and 1265.17 cm^{-1} for the wagging mode in Figure 1. The C-H stretching modes at around 3100 cm^{-1} calculated by ORCA are barely visible in Figure 1.

3.3.2 Raman

The measured Raman spectrum of dichloromethane is shown in Figure 2, plotting the Raman intensity against the Raman shift $\Delta\tilde{\nu}$.

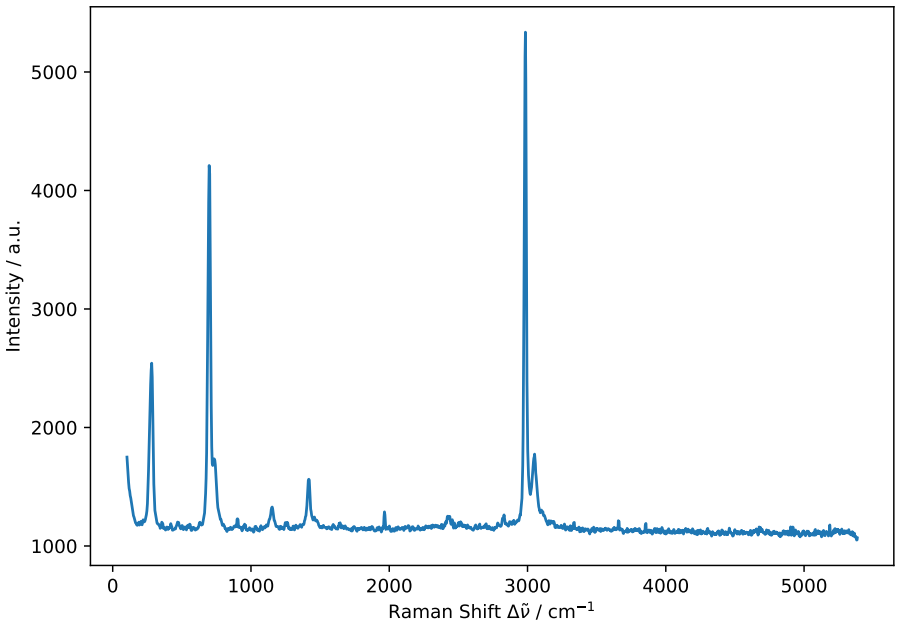

Fig. 2: Measured raman spectrum of dichloromethane.

By visual inspection of the Raman spectrum in Figure 2, five primary absorption signals can be identified, which are listed with their corresponding Raman shift, Raman intensity and vibration type of each mode.

Tab. 7: Listed are the measured Raman shifts and intensities of the signals of CH_2Cl_2.

Signal	Raman shift $\Delta\tilde{\nu}$ / cm^{-1}	intensity / a.u.	Vibration type
1	281.99	2542.67	scissoring
2	697.77	4210.67	sym. stretching
3	1418.07	1563.33	scissoring
4	2984.85	5336.00	sym. stretching
5	3051.13	1775.33	asym. stretching

The simulated Raman-active vibrational modes of dichloromethane are summarized in Table 8 with the corresponding Raman shift, Raman intensity and vibration type of each mode.

Tab. 8: Listed are the simulated Raman shifts and intensities of the vibrational modes of CH_2Cl_2.

Mode	Raman Shift $\Delta\tilde{\nu}$ / cm^{-1}	Raman intensity / $Å^4$ amu^{-1}	Vibration type
1	277.06	6.83	scissoring
2	703.48	12.27	sym. stretching
3	732.67	5.02	asym. stretching
4	888.90	3.13	-
5	1153.83	11.78	-
6	1272.67	3.01	-
7	1441.64	12.42	scissoring
8	3106.65	108.70	sym. stretching
9	3193.09	62.65	asym. stretching

As can be seen in Table 7, the most intense Raman-active modes are found at wavenumbers of 281.99 cm^{-1}, 697.77 cm^{-1} and 2984.85 cm^{-1}, which correspond to the calculated signals at 277.06 cm^{-1} for the scissoring mode and 703.48 cm^{-1} for the symmetric stretching mode in Table 8. But similar to the IR spectrum, the wavenumbers of the C-H stretching modes in the measured Raman spectrum at 2984.85 cm^{-1} and 3051.13 cm^{-1} deviate by approximately 130 cm^{-1} from the calculated values of 3106.65 cm^{-1} and 3193.09 cm^{-1}.

3.4 Dibromomethane

3.4.1 IR

The measured IR spectrum of dibromomethane is shown in Figure 3, plotting the intensity of the absorption against the wavenumber $\tilde{\nu}$.

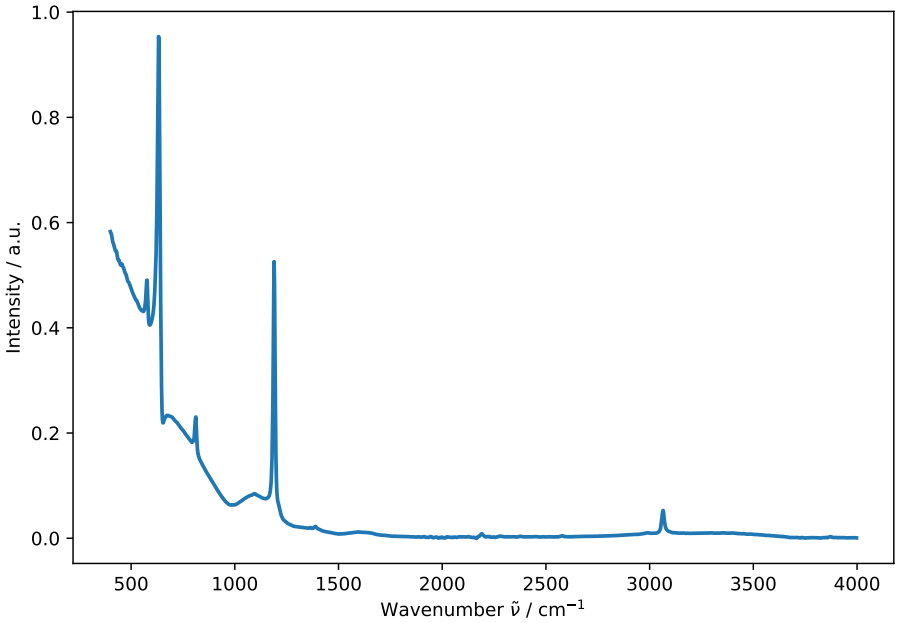

Fig. 3: Measured IR spectrum of dibromomethane.

By visual inspection of the IR spectrum in Figure 3, six absorption signals can be identified, which are listed with their corresponding wavenumbers and intensities in Table 9.

Tab. 9: Listed are the measured wavenumbers and intensities of the IR signals of CH_2Br_2.

Signal	Wavenumber $\tilde{\nu}$ / cm^{-1}	Intensity / a.u.	vibration type
1	455.05	0.52	-
2	577.49	0.49	C−Br sym. stretching
3	632.58	0.95	C−Br asym. stretching
4	677.48	0.23	-
5	812.16	0.23	rocking
6	1095.80	0.08	twisting
7	1189.66	0.53	wagging
8	1389.64	0.02	scissoring
11	3064.97	0.05	-

The simulated vibrational modes of dibromomethane are summarized in Table 10 with the corresponding wavenumber, intensity and vibration type of each mode.

Tab. 10: Listed are the simulated wavenumbers and intensities of the vibrational modes of CH_2Br_2.

Mode	Wavenumber $\tilde{\nu}$ / cm^{-1}	Intensity / $KM{\cdot}mol^{-1}$	vibration type
1	168.72	0.08	C−Br scissoring
2	573.58	4.08	C−Br sym. stretching
3	628.31	98.95	C−Br asym. stretching
4	806.07	4.64	rocking
5	1101.92	0.00	twisting
6	1205.80	65.32	wagging
7	1412.95	0.00	scissoring
8	3126.16	1.92	sym. stretching
9	3221.84	1.28	asym. stretching

As Table 10 shows, the most intense IR-active modes are found at wavenumbers of 628.31 cm^{-1} and 1205.80 cm^{-1}, which correspond well to the measured signals at 632.58 cm^{-1} for the C−Br asymmetric stretching mode and at 1189.66 cm^{-1} for the wagging mode. The comparison of the two tables also shows that although the twisting mode and scissoring mode should not be IR-active they still show up in the spectrum.

3.4.2 Raman

The measured Raman spectrum of dibromomethane is shown in Figure 4, plotting the Raman intensity against the Raman shift $\Delta\tilde{\nu}$.

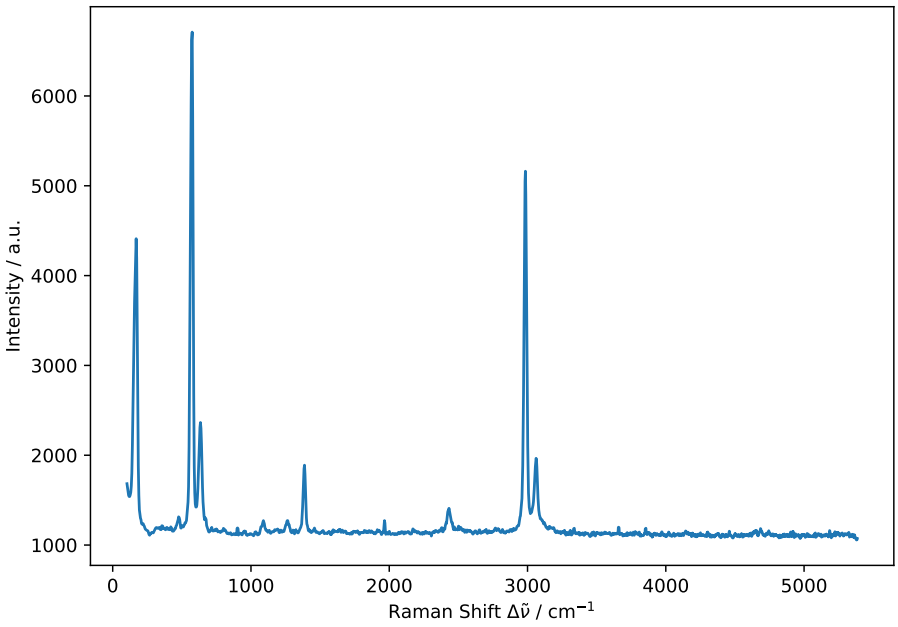

Fig. 4: Measured raman spectrum of dibromomethane.

By visual inspection of the Raman spectrum in Figure 4, seven primary absorption signals can be identified, which are listed with their corresponding Raman shift, Raman intensity and vibration type of each mode.

Tab. 11: Listed are the measured Raman shifts and intensities of the signals of CH_2Br_2.

Signal	Raman shift $\Delta\tilde{\nu}$ / cm^{-1}	Intensity / a.u.	vibration type
1	169.61	4410.67	C−Br scissoring
2	574.79	6711.00	C−Br sym. stretching
3	634.60	2364.33	C−Br asym. stretching
4	1387.16	1889.33	scissoring
5	2432.07	1409.00	-
6	2984.85	5162.00	sym. stretching
7	3062.11	1965.67	asym. stretching

The simulated Raman-active vibrational modes of dibromomethane are summarized in Table 12 with the corresponding Raman shift, Raman intensity and vibration type of each mode.

Tab. 12: Listed are the simulated wavenumbers and raman intensities of the vibrational modes of CH_2Br_2.

Mode	Wavenumber $\tilde{\nu}$ / cm^{-1}	Raman intensity / $Å^4$ amu^{-1}	vibration type
1	168.56	5.37	C−Br scissoring
2	574.64	13.43	C−Br sym. stretching
3	629.71	5.36	C−Br asym. stretching
4	806.60	2.41	rocking
5	1102.17	8.43	twisting
6	1205.71	0.74	wagging
7	1413.22	13.77	scissoring
8	3125.63	97.24	sym. stretching
9	3221.31	58.05	asym. stretching

As Table 12 shows, the most intense raman-active modes are found at wavenumbers of 3125.63 cm^{-1} and 3221.31 cm^{-1}, which correspond to the measured signals at 2984.85 cm^{-1} for the symmetric stretching mode and at 3062.11 cm^{-1} for the asymmetric stretching mode. That means that the symmetric and asymmetric stretching of the C−H bonds is the most raman active type of vibration.

3.5 Chloroform

3.5.1 IR

The measured IR spectrum of chloroform is shown in Figure 5, plotting the intensity of the absorption against the wavenumber $\tilde{\nu}$.

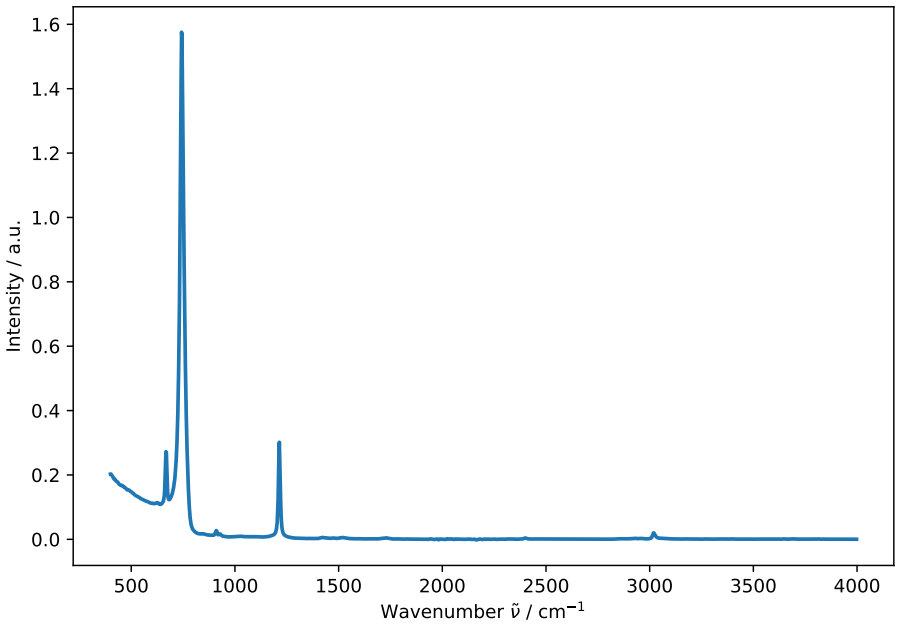

Fig. 5: Measured IR spectrum of chloroform.

By visual inspection of the IR spectrum in Figure 5, three absorption signals can be identified, which are listed with their corresponding wavenumbers and intensities in Table 13.

Tab. 13: Listed are the measured wavenumbers and intensities of the IR signals of $CHCl_3$.

Signal	Wavenumber $\tilde{\nu}$ / cm^{-1}	Intensity / a.u.	vibration type
1	626.46	0.11	-
2	667.27	0.27	C−Cl sym. stretching
3	742.78	1.58	C−Cl asym. stretching
4	910.10	0.03	-
5	928.47	0.02	-
6	1214.15	0.30	bending
7	3020.07	0.02	sym. stretching

The simulated vibrational modes of chloroform are summarized in Table 14 with the corresponding wavenumber, intensity and vibration type of each mode.

Tab. 14: Listed are the simulated wavenumbers and intensities of the vibrational modes of $CHCl_3$.

Mode	Wavenumber $\tilde{\nu}$ / cm^{-1}	Intensity / $KM{\cdot}mol^{-1}$	vibration type
1	254.78	0.06	C−Cl scissoring
2	254.97	0.06	C−Cl scissoring
3	362.33	0.46	C−Cl scissoring
4	665.85	7.26	C−Cl sym. stretching
5	741.92	167.74	C−Cl asym. stretching
6	742.13	167.67	C−Cl asym. stretching
7	1220.08	22.80	bending
8	1220.17	22.76	bending
9	3169.43	0.22	sym. stretching

As Table 14 shows, the most intense IR-active modes are found at wavenumbers of 741.92 cm^{-1} and 742.13 cm^{-1}, which correspond to the measured signal at 742.78 cm^{-1} for the C−Cl asymmetric stretching mode. That means that the asymmetric stretching of the C−Cl bond is the most IR active type of vibration. It is to be noted, that the simulation showed two distinct vibrational modes, while the measurement only shows one mode. The simulated bending modes at 1220.08 cm^{-1} and 1220.17 cm^{-1} that show the second highest intensities, were also measured as only one signal at 1214.15 cm^{-1}.

3.5.2 Raman

The measured Raman spectrum of chloroform is shown in **??**, plotting the Raman intensity against the Raman shift $\Delta\tilde{\nu}$.

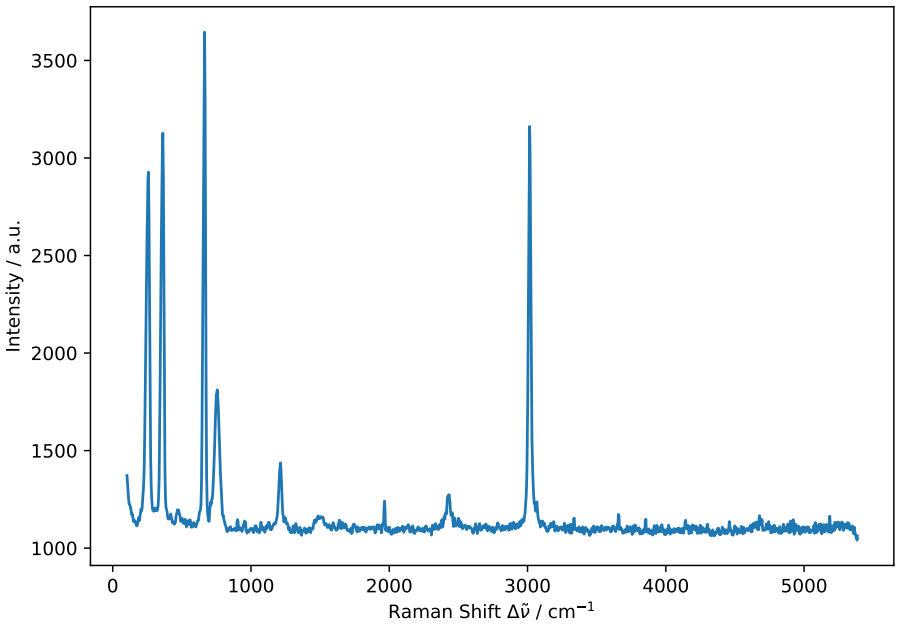

Fig. 6: Measured raman spectrum of chloroform.

By visual inspection of the Raman spectrum in Figure 6, six primary absorption signals can be identified, which are listed with their corresponding Raman shift, Raman intensity and vibration type of each mode.

Tab. 15: Listed are the measured Raman shifts and intensities of the signals of $CHCl_3$.

Signal	Raman shift $\Delta\tilde{\nu}$ / cm^{-1}	Intensity / a.u.	vibration type
1	258.84	2927.00	C−Cl scissoring
2	362.65	3127.33	C−Cl scissoring
3	664.38	3645.00	C−Cl sym. stretching
4	756.86	1811.33	C−Cl asym. stretching
5	1213.44	1437.33	bending
6	3015.32	3161.67	sym. stretching

The simulated Raman-active vibrational modes of chloroform are summarized in Table 16 with the corresponding Raman shift, Raman intensity and vibration type of each mode.

Tab. 16: Listed are the simulated wavenumbers and raman intensities of the vibrational modes of $CHCl_3$.

Mode	Wavenumber $\tilde{\nu}$ / cm^{-1}	Raman intensity / $Å^4$ amu^{-1}	vibration type
1	254.60	5.14	C−Cl scissoring
2	255.07	5.13	C−Cl scissoring
3	362.22	8.69	C−Cl scissoring
4	665.69	9.80	C−Cl sym. stretching
5	740.88	3.08	C−Cl asym. stretching
6	741.45	3.07	C−Cl asym. stretching
7	1220.22	6.04	bending
8	1220.68	6.05	bending
9	3168.77	77.28	sym. stretching

As Table 16 shows, the most intense raman-active mode is found at the wavenumber 3168.77 cm^{-1}, which corresponds to the measured signal at 3015.32 cm^{-1} for the symmetric stretching mode. That means that the symmetric stretching of the C−H bond is the most raman active type of vibration. Even though the C−Cl vibrational modes should not be nearly as intense as the symmetric stretching mode, they almost equal the simulated values.

3.6 Deuterated Chloroform

3.6.1 IR

Tab. 17: Listed are the simulated wavenumbers and intensities of the vibrational modes of $CDCl_3$.

Mode	Wavenumber $\tilde{\nu}$ / cm^{-1}	Intensity / KM·mol^{-1}	vibration type
1	253.69	0.06	C−Cl scissoring
2	253.88	0.06	C−Cl scissoring
3	360.12	0.50	C−Cl scissoring
4	646.14	6.66	C−Cl sym. stretching
5	717.83	125.46	C−Cl asym. stretching
6	717.98	125.28	C−Cl asym. stretching
7	909.65	63.16	bending
8	909.66	63.19	bending
9	2342.61	0.74	sym. stretching

3.6.2 Raman

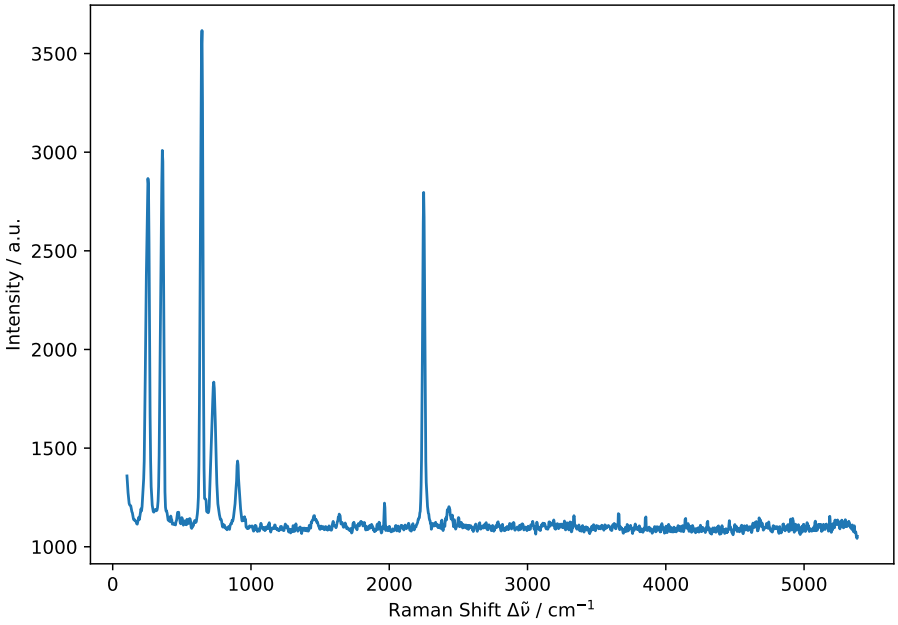

Fig. 7: Measured raman spectrum of deuterated chloroform.

Tab. 18: Listed are the measured Raman shifts and intensities of the signals of $CDCl_3$.

Signal	Raman shift $\Delta\tilde{\nu}$ / cm^{-1}	Intensity / a.u.
1	254.97	2866.67
2	358.83	3009.00
3	645.78	3616.67
4	731.05	1834.67
5	903.05	1434.67
6	2248.93	2796.00

Tab. 19: Listed are the simulated wavenumbers and raman intensities of the vibrational modes of $CDCl_3$.

Mode	Wavenumber $\tilde{\nu}$ / cm^{-1}	Raman intensity / $Å^4$ amu^{-1}	vibration type
1	253.69	0.06	C−Cl scissoring
2	253.88	0.06	C−Cl scissoring
3	360.12	0.50	C−Cl scissoring
4	646.14	6.66	C−Cl sym. stretching
5	717.83	125.46	C−Cl asym. stretching
6	717.98	125.28	C−Cl asym. stretching
7	909.65	63.16	bending
8	909.66	63.19	bending
9	2342.61	0.74	sym. stretching

3.7 Tetrachloromethane

3.7.1 IR

Tab. 20: Listed are the simulated wavenumbers and intensities of the vibrational modes of CCl_4.

Mode	Wavenumber $\tilde{\nu}$ / cm^{-1}	Intensity / KM·mol^{-1}	vibration type
1	212.71	0.00	scissoring
2	212.89	0.00	scissoring
3	310.72	0.06	scissoring
4	310.82	0.06	scissoring
5	310.88	0.06	scissoring
6	451.20	0.00	sym. stretching
7	754.80	185.52	asym. stretching
8	755.02	185.61	asym. stretching
9	755.51	185.58	asym. stretching

3.7.2 Raman

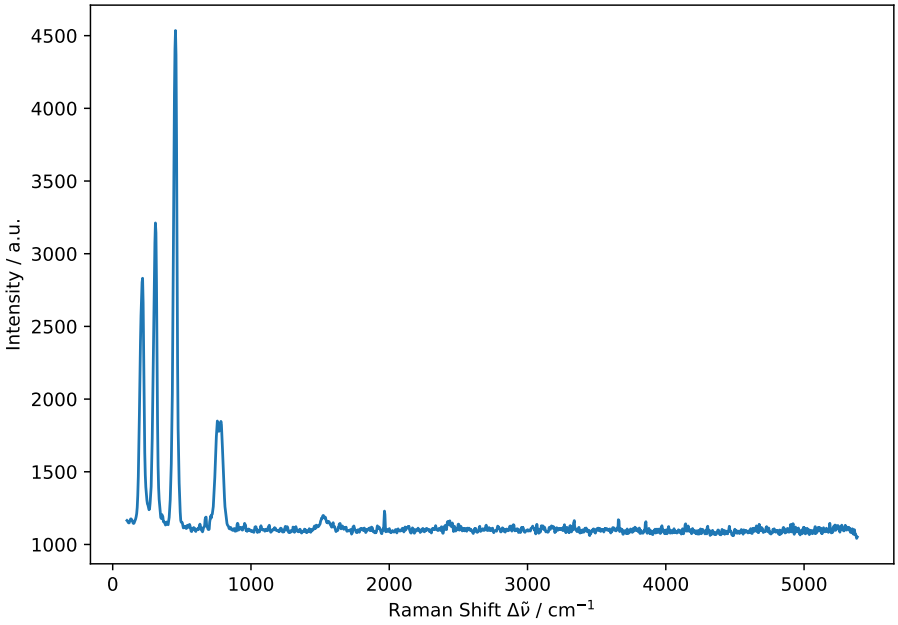

Fig. 8: Measured raman spectrum of tetrachloromethane.

Tab. 21: Listed are the measured Raman shifts and intensities of the signals of CCl_4.

Signal	Raman shift $\Delta\tilde{\nu}$ / cm^{-1}	Intensity / a.u.
1	216.25	2831.33
2	308.95	3211.67
3	454.10	4535.33
4	756.86	1849.33

Tab. 22: Listed are the simulated wavenumbers and Raman intensities of the vibrational modes of CCl_4.

Mode	Wavenumber $\tilde{\nu}$ / cm^{-1}	Raman intensity / $Å^4$ amu^{-1}	vibration type
1	212.71	4.18	scissoring
2	212.91	4.17	scissoring
3	310.52	5.39	scissoring
4	310.84	5.40	scissoring
5	311.16	5.40	scissoring
6	451.08	16.40	sym. stretching
7	753.44	1.55	asym. stretching
8	754.26	1.56	asym. stretching
9	754.60	1.54	asym. stretching

3.8 Tetrachloroethylene

3.8.1 IR

The measured IR spectrum of tetrachloroethylene is shown in Figure 9, plotting the intensity of the absorption against the wavenumber $\tilde{\nu}$.

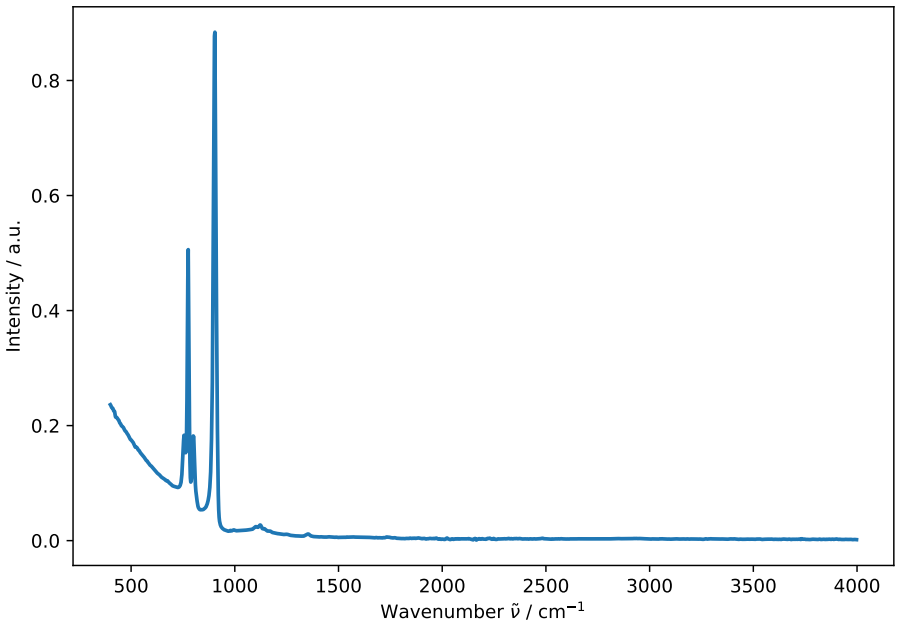

Fig. 9: Measured IR spectrum of tetrachloroethylene.

By visual inspection of the IR spectrum in Figure 9, six absorption signals can be identified, which are listed with their corresponding wavenumbers and intensities in Table 23.

Tab. 23: Listed are the measured wavenumbers and intensities of the IR signals of C_2Cl_4 with the corresponding type of the vibrational mode.

Signal	Wavenumber $\tilde{\nu}$ / cm^{-1}	Intensity / a.u.	Vibration type
1	755.02	0.18	-
2	775.42	0.51	asym. C-Cl stretching
3	799.91	0.18	-
4	903.98	0.88	asym. C-Cl stretching
5	1122.32	0.03	-
6	1354.95	0.01	-

The simulated vibrational modes of tetrachloroethylene are summarized in Table 24 with the corresponding wavenumber, intensity and vibration type of each mode.

Tab. 24: Listed are the simulated wavenumbers and intensities of the vibrational modes of C_2Cl_4.

Mode	Wavenumber $\tilde{\nu}$ / cm^{-1}	Intensity / $KM \cdot mol^{-1}$	Vibration type
1	97.18	0.00	twisting
2	174.89	0.96	scissoring
3	234.77	0.00	scissoring
4	286.90	0.51	wagging
5	310.42	0.03	scissoring
6	342.99	0.00	asym. bending
7	447.02	0.00	sym. stretching
8	514.19	0.00	wagging
9	774.46	82.16	asym. stretching
10	895.52	202.05	asym. stretching
11	978.50	0.00	asym. stretching
12	1624.06	0.00	C = C stretching

As can be seen in Table 24, the most intense IR-active modes are found at wavenumbers of 774.46 cm^{-1} and 895.52 cm^{-1}, which correspond well to the measured signals at 755.02 cm^{-1} and 903.98 cm^{-1} in Figure 9. The signals at 755.02 cm^{-1} and 799.91 cm^{-1} can be assumed to occur due to isotopic effects, as chlorine has two stable isotopes, ^{35}Cl and ^{37}Cl, leading to small shifts in the vibrational frequencies. The two signals above 1100 cm^{-1} may indicate overtones or combination bands, which are weaker in intensity compared to the fundamental normal modes.

In comparison to the simulated IR spectrum of chloroform with the wavenumbers and vibrational modes in Table 13, tetrachloroethylene shows additional IR-active modes in the low wavenumber region below 500 cm^{-1}, which can be attributed to the increased number of atoms in the molecule leading to more vibrational modes.

3.8.2 Raman

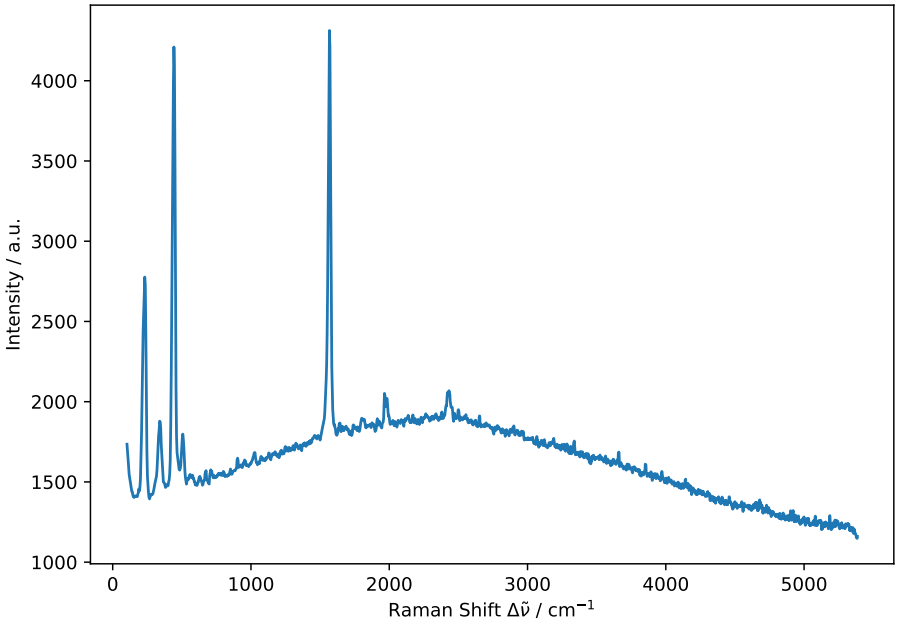

Fig. 10: Measured raman spectrum of tetrachloroethylene.

Tab. 25: Listed are the measured Raman shifts and intensities of the signals of C_2Cl_4.

Signal	Raman shift $\Delta\tilde{\nu}$ / cm^{-1}	Intensity / a.u.	Vibration type
1	231.76	2776.67	scissoring
2	339.67	1879.00	asym. bending
3	442.71	4210.33	sym. stretching
4	1567.61	4313.00	C = C stretching
5	2432.07	2068.33	-

Tab. 26: Listed are the simulated wavenumbers and Raman intensities of the vibrational modes of C_2Cl_4.

Mode	Wavenumber $\tilde{\nu}$ / cm^{-1}	Raman intensity / $Å^4$ amu^{-1}	Vibration type
1	97.98	0.00	twisting
2	174.79	0.00	scissoring
3	234.62	5.56	scissoring
4	289.22	0.00	wagging
5	310.02	0.00	scissoring
6	342.83	4.61	asym. bending
7	446.81	15.61	sym. stretching
8	517.38	3.22	wagging
9	774.24	0.00	asym. stretching
10	895.62	0.00	asym. stretching
11	978.54	0.44	asym. stretching
12	1623.90	48.63	C = C stretching

In comparison to the simulated IR-active modes in Table 24, Table 26 shows that the most intense Raman-active mode is found at a wavenumber of 1623.90 cm^{-1}, which can be assigned to the C = C stretching mode of tetrachloroethylene, which is not present in the simulated IR spectrum. The cause for this lies in the rule of mutual exclusion, which applies to molecules with a center of symmetry, such as the inversion center of tetrachloroethylene. According to this rule, vibrational modes that are Raman-active are IR-inactive and vice versa, explaining the absence of the 1623.90 cm^{-1} mode in the IR spectrum. By comparing the simulated Raman modes of C_2Cl_4 from Table 26 with the simulated Raman modes of $CHCl_3$ in Table 15, the structural differences between the two molecules can be explained. While both molecules show Raman-active modes in the low wavenumber region below 500 cm^{-1}, tetrachloroethylene exhibits an additional strong Raman-active mode at 1623.90 cm^{-1}, which can be attributed to the presence of the C = C double bond in C_2Cl_4 that is absent in $CHCl_3$. Additionally, the C-H stretching mode at 3168.77 cm^{-1} present in chloroform is not observed in tetrachloroethylene due to the lack of hydrogen atoms in its structure.

4 Discussion

By plotting the calculated Raman shifts against the vibrational mode number for Methane and all Chloromethanes from Table 2, Table 4, Table 8, Table 16 and Table 22, the Raman trends of the investigated molecules can be visualized in Figure 11.

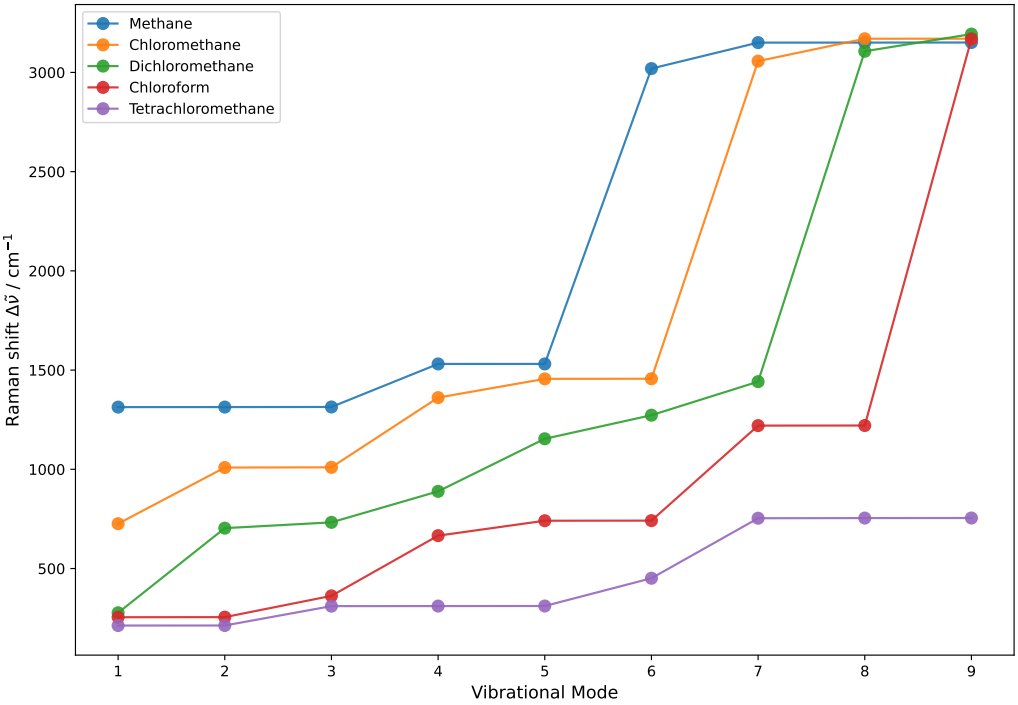

Fig. 11: Raman shifts plotted against the vibrational mode number for CH_4, CH_3Cl, CH_2Cl_2, $CHCl_3$ and CCl_4.

The first trend noticeable in Figure 11 is the decrease of the Raman shifts with increasing number of chlorine atoms in the molecule. This can be explained by the increasing reduced mass μ of the molecules due to the substitution of hydrogen atoms (mass = 1 u) with chlorine atoms (mass = 35.5 u), leading to lower vibrational frequencies $\tilde{\nu}$ according to Equation 1.

$$\tilde{\nu} = \nu \cdot c = \sqrt{\frac{k}{\mu}} \tag{1}$$

Following that argumentation, the number of vibrational modes at around 3000 cm^{-1}, which can be assigned to the C-H stretching vibrations, decreases with increasing number of chlorine atoms in the molecule until no C-H stretching modes are present in tetrachloromethane due to the absence of hydrogen atoms in its structure. In return, new vibrational modes appear in the low wavenumber region below 1000 cm^{-1}, which can be assigned to the C-Cl stretching vibrations. Another trend observable in Figure 11 is that methane and tetrachloromethane show more vibrational modes with nearly the same Raman shift compared to the other chloromethanes. This can be explained by the high symmetry of both molecules, which belong to the tetrahedral point group T_d. This trend is especially visible in the triply degenerate asymmetric stretching vibration of methane at 3150 cm^{-1} and tetrachloromethane at 754 cm^{-1}.

5 Conclusion

6 References

[1] H. Dilger, *2025-pc2-script-en*, **2025**.